Ocean Science

# Seasonality of intermediate waters hydrography west of the Iberian Peninsula from an 8 yr semiannual time series of an oceanographic section

E. Prieto[1], C. González-Pola[1], A. Lavín[2], R. F. Sánchez[3], and M. Ruiz-Villarreal[4]

[1]Spanish Institute of Oceanography, Oceanographic Centre of Gijón, Gijón, Spain
[2]Spanish Institute of Oceanography, Oceanographic Centre of Santander, Santander, Spain
[3]Spanish Institute of Oceanography, Oceanographic Centre of Cádiz, Cádiz, Spain
[4]Spanish Institute of Oceanography, Oceanographic Centre of A Coruña, A Coruña, Spain

*Correspondence to:* E. Prieto (eva.prieto@gi.ieo.es)

**Abstract.** Seasonality of hydrographical properties at depth in the western Iberian margin (eastern North Atlantic) is analysed from a 2003–2010 time series of a semiannual oceanographic section extending $\sim 200$ nm off Cape Finisterre (43° N). All water masses down to the permanent thermocline (2000 dbar) show a consistent seasonal signature in their thermohaline properties and there is a notable asymmetry between the slope region and the outer ocean (in the surroundings of the Galicia Bank). There is overall cooling and freshening of eastern North Atlantic central waters in summertime, which is larger and deeper-reaching on the slope. In summertime, Mediterranean Water (MW) gets tightly attached against the slope and is uplifted, reinforcing its thermohaline signature and diminishing its presence at the outer ocean. In wintertime the situation reverses, MW seems to detach from the slope and spreads out to the open ocean, even being observed a secondary branch around the Galicia Bank. Thermohaline seasonality at depth shows values up to 0.4 °C and 0.08 in salinity at the lower MW, of the order of 20 % of the overall interannual variability observed during the whole period. Decomposition of thermohaline changes at isobaric levels to changes along isoneutral surfaces and changes due to vertical displacements help analyse the physical processes behind the observed seasonality in terms of (1) the large-scale seasonality of the subtropical gyre in response to the seasonal migration of the subtropical high pressure system and subsequent anomalies in Ekman transport and wind stress curl, (2) the continental slope dynamics, characterized by summer upwelling, winter development of the Iberian Poleward Current and Mediterranean water spreading, and (3) the possible influence of seasonal changes of water mass properties at their formation sources.

## 1 Introduction

The ocean is a crucial component of Earth's climate, playing a key role in the regulation of global energy budget by transporting heat and salt from low to high latitudes and storing large amounts of heat and carbon dioxide. Understanding of the climate system and its current evolution under a climate change scenario requires precise knowledge on the spatial and temporal scales of variability of water mass properties and major current systems. Such a task makes necessary the establishment of long-term monitoring programs to observe the ocean variability.

There exists a large number of studies dealing with trends and interannual variability of water mass properties, stating widespread warming since at least the second half of the 20th century (e.g. Solomon et al., 2007). However, information about seasonal fluctuations in the ocean interior is less robust and more scarce, due to the lack of subannual monitoring programs, adding a potential source of noise when trying to solve climatic trends. Seasonality in water mass properties and current fields are expected as a response of the yearly heating/cooling cycle and the large-scale response in

the wind curl, and evidence of seasonal variability below the seasonal thermocline has long ago been anticipated theoretically (e.g. Krauss and Wuebber, 1982, for the case of the North Atlantic). Recently Chidichimo et al. (2010) and Kanzow et al. (2010) reported a strong contribution of the eastern boundary density variations in the subtropical Atlantic to subseasonal and seasonal anomalies in the strength and vertical structure of the Atlantic meridional overturning.

In the present contribution, we exploit a dataset of semi-annual occupations of a hydrographic section located further north (43° N, 009–014° W, off Cape Finisterre, west of the Iberian Peninsula), to explore the seasonal variability of water masses below the mixed layer in the midlatitude eastern boundary of the North Atlantic. Section 2 introduces the dataset and provides a framework for the sections by providing a brief description of the local hydrography and circulation patterns. Section 3 presents the methodology, while in Sect. 4 patterns of seasonality are characterized. The possible causes of seasonality at different levels are then discussed in Sect. 5 in relationship to the eastern boundary of the subtropical gyre dynamics, slope currents and water mass formation processes. Finally, Sect. 6 summarizes the main conclusions of the work.

## 2 Regional oceanographical framework and dataset

### 2.1 Water masses and circulation west of the Iberian Peninsula

The western Iberian margin is a portion of the North Atlantic eastern boundary located at the north-eastern edge of the subtropical gyre. Upper ocean circulation is weak, exhibiting a mean southward flow of few cm s$^{-1}$ (Mazé et al., 1997; Paillet and Mercier, 1997), but dominated by mesoscale activity (Memery et al., 2005). The continental slope is characterized by the development of a density driven countercurrent (poleward) known as the Iberian Poleward Current, IPC (e.g. Frouin et al., 1990; Peliz et al., 2005). A detailed review of the modal, intermediate and deep water masses of the midlatitude north-east Atlantic Ocean was performed by van Aken (2000a,b, 2001) and sketches of the pathways of such waters masses from their source region towards western Iberia are shown in Fig. 1a. Briefly, these are as follows:

- Eastern North Atlantic Central Water (ENACW) constitutes the upper permanent thermocline of the European and north-west African basins. It is characterized by a narrow and nearly straight line in the $\theta/S$ with its core located at ∼ 350 dbar. ENACW is formed by winter mixing in a wide region from the Azores to the European boundary bounded by the North Atlantic Current (NAC) and the Azores Current (AC) (Pollard and Pu, 1985; Pollard et al., 1996). In the western Iberia margin, warmer ENACW of subtropical origin created near the Azores flows eastward and mixes with the colder south-

ward flowing ENACW of subpolar origin (Fiúza et al., 1998). The lower bound of ENACW is characterized by a salinity minimum.

- Mediterranean Water (MW) is formed at the Gulf of Cádiz from the intense mixing of Atlantic central waters and the warm and salty overflow from the Mediterranean Sea through the Strait of Gibraltar. The main core is characterized by a clear salinity maximum spreading from Cape St. Vincent at 37° N as a northward deep boundary current along the European ocean margin, and reaching high latitudes as the Porcupine Bank at 53° N. Along the west Iberian margin, two cores are found: the upper (MW$_u$) at ∼ 750 dbar and the lower (MW$_l$) at ∼ 1250 dbar, becoming indistinguishable north of 42° N. West of Cape Finisterre, an intermediate salinity maximum centered at 1000 dbar is observed between a salinity minimum at about 500 dbar and a minimum connected with the below-lying Labrador Sea Water (LSW) core near 1900 dbar (Iorga and Lozier, 1999b; van Aken, 2000b).

- Labrador Sea Water (LSW) is the deeper intermediate water mass (i.e. belonging to the permanent thermocline). It is the last stage of the modification of the subpolar gyre mode waters formed in the centre of the cyclonic circulation in the Labrador Sea by deep winter convection, spreading southwards and eastwards in the North Atlantic from its formation area. In the north-east Atlantic, its core is characterized by a deep salinity minimum near 1900 dbar (Pingree, 1973).

- Eastern North Atlantic Deep Water (ENADW), found below the intermediate water masses, is formed by a mixture of different polar source water types including a component of Antarctic origin (van Aken, 2000a). The term Lower Deep Water (LDW) is used for the bottom waters found deeper than 4000 m.

### 2.2 The VACLAN/COVACLAN projects

An intense monitoring program of the ocean hydrography in the Bay of Biscay and western Iberia margin has been taking place since the year 2003 (project VACLAN-Climate Variability in the eastern North Atlantic – of the Spanish Institute of Oceanography, http://www.vaclan-ieo.es/). The aim of the program is the maintenance of a permanent observation system of the ocean climate variability in this region of the north-east Atlantic Ocean, through the assessment of changes in physico-chemical properties and circulation patterns of the ocean. Hydrography and chemistry of the whole water column were sampled twice a year, in winter- and summertime, for the period 2003–2010 at three oceanic sections perpendicular to the coast, two in the Bay of Biscay and one at the western Iberian margin at 43° N
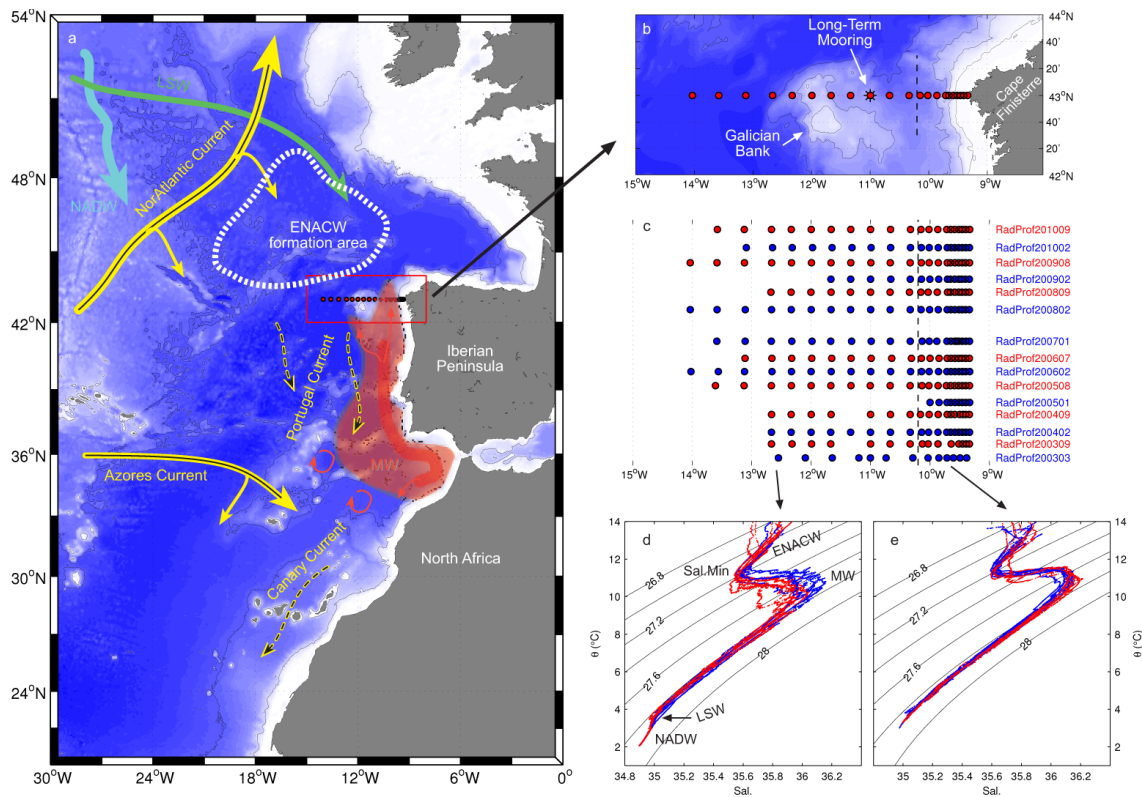
**Fig. 1. (a)** Plate summarising the main circulation patterns of waters in the area and the Finisterre section. Gyres bounding North Atlantic Current (NAC) and Azores Current (AC) (yelow bold), southward flowing Portugal Current (PC) and Canary Current (CC) (yellow dashed). Central water: ENACW formation area is shown as a dashed white region north of Finisterre, from where it flows southwards with the PC. Intermediate waters: Mediterranean water (MW, red), spreading from the Strait of Gibraltar, flows northwards along the continental slope sometimes showing a detachment contouring the west Galicia Bank, and southward flowing water from the Labrador Sea (LSW, green). North Atlantic Deep Water (NADW, blue). **(b)** Zoom of the Finisterre section. **(c)** Graphical representation of the hydrographical database. Dots are plotted at true positions with reference to **(b)**. Blue cruises are for winter and red for summer. **(d)** $\theta S$ diagram of all profiles at a station 012°40′ W, west of the Galicia Bank (colours keep to represent winter vs summer profiles). **(e)** Same as **(d)** for a slope station 009°43′ W.

($\sim$ 200 nm off Cape Finisterre). This latter section supports the present contribution.

The cruises consist of standard hydrography performed by SBE911 + CTD (Seabird; conductivity-temperature-depth) bathysondes provided with redundancy in conductivity and temperature and some additional sensors (oximeter, turbidimeter and fluorometer), integrated into an oceanographic rosette. Water samples are used to analyse nutrients and to calibrate salinity (with Guideline Autosal 8400 B salinometers) and $O_2$ sensors. The study presented here is based on the hydrographical database collected in fifteen surveys performed in the 2003–2010 period within the Finisterre (43° N) section (Fig. 1b).

Orography in this region is characterized by a narrow continental shelf of about $\sim$ 25 km, a steep slope and the presence of a seamount about 200 km west of the coast of Galicia (the "Galicia Bank"), which has a great impact on circulation patterns and marine biodiversity in the region (e.g. Ruiz-Villarreal et al., 2006). An inventory of the surveys is shown

in Table 1 and Fig. 1c. The 8-yr-long record provides a sufficient database to explore the presence of seasonality at depth in the region and to characterize it, which is the purpose of the present contribution. Figures 1d and e show the $\theta S$ diagram at two stations, one well in the basin west of the Galicia Bank and the other on the slope, showing the signature of the water masses described in Sect. 2.1 and providing a first suggestion of a distinct pattern between summer and winter profiles, specially seen in the signature of Mediterranean Water.

## 3 Methods

The first step in order to quantify the seasonality in the different waters masses is to adopt a systematic and objective classification of them. Water masses are distributed as layers with distinct hydrographical properties placed approximately at specific depths. Normally, water masses are labelled by characteristic density levels, while depth is only

**Table 1.** VACLAN/COVACLAN series of cruises ("RadProf" is an acronym for the Spanish of "Deep Section"). Dates and stations sampled at Finisterre section indicating those sampled at the shelf-slope ($N_I$: 43° N, 009.2–010.2° W) and open ocean region ($N_{II}$: 43° N, 010.2–014.0° W).
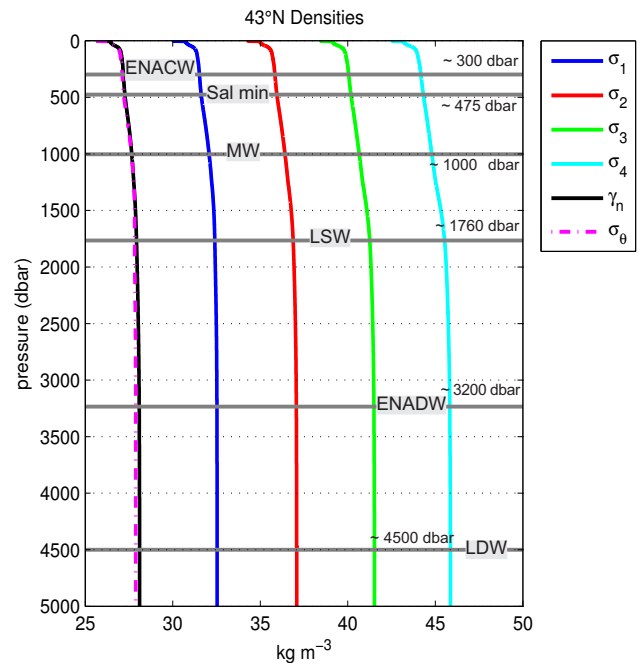
| Cruise | dates | $N_I$ (Slope) | $N_{II}$ (Outer) |
|---|---|---|---|
| RadProf200303 | 26 March–17 April 2003 | 6 | 7 |
| RadProf200309 | 10–20 September 2003 | 8 | 8 |
| RadProf200402 | 5–13 February 2004 | 10 | 8 |
| RadProf200409 | 7–13 September 2004 | 10 | 8 |
| RadProf200501 | 27 January–3 February 2005 | 6 | – |
| RadProf200508 | 20 August–9 September 2005 | 10 | 9 |
| RadProf200602 | 5–13 February 2006 | 10 | 9 |
| RadProf200607 | 12–29 July 2006 | 10 | 9 |
| RadProf200702 | 1–7 February 2007 | 11 | 9 |
| Ship unavailable | – | – | – |
| RadProf200802 | 11–19 February 2008 | 10 | 9 |
| RadProf200809 | 3–13 September 2008 | 10 | 8 |
| RadProf200902 | 1–13 February 2009 | 10 | 5 |
| RadProf200908 | 11–21 August 2009 | 10 | 9 |
| RadProf201002 | 9–11 February 2010 | 10 | 9 |
| RadProf201009 | 2–11 September 2010 | 10 | 9 |



**Fig. 2.** Time and zonally averaged potential density relative to the sea surface ($\sigma_\theta$), 1000 dbar, 2000 dbar, 3000 dbar, 4000 dbar ($\sigma_{1,2,3,4}$) and neutral density ($\gamma^n$) as a function of pressure.

taken as reference below the permanent thermocline where density gradient is very weak. The most detailed description of the water masses in the midlatitude north-east Atlantic (van Aken, 2000a,b, 2001) used isopycnal bounds to tag the main water masses referred to in Sect. 2.1, with the exception of LDW identified with deep water located roughly below 4000 dbar. We have followed these works in order to label the water masses, with the exception of ENACW and salinity minimum, which have been identified focusing on the $\theta/S$ diagrams of Figs. 1d and e, but using neutral density $\gamma^n$ (Jackett and McDougall, 1997) instead of potential density. Table 2 summarizes water mass properties from density levels and corresponding depth-averaged pressure providing also potential temperature and salinity averages at the 43° N section. Figure 2 provides a graphical view of the water masses division.

Different behaviour is expected on the slope or further into the basin, and actually a distinct pattern emerges from a first glance of the dataset (see Fig. 1d, e). For this reason, the section will be divided into two subsections (see Fig. 1b) with the aim of studying the seasonality separately. These are:

1. The *slope*, which extends from the Galicia coast off Cape Finisterre at ∼ 9.3° W to the middle of the trough at 10.2° W.

2. The *outer ocean*, which spans from 10.2° W to 14° W, hence including the Galicia Bank.

In order to analyse water mass changes, it is helpful to consider separately thermohaline changes occurring at fixed density levels (hence causing a true modification of the $\theta S$ diagram) and vertical displacement of isopycnal levels (a process known as heave). Properties of modal waters formation are set by the balances in atmospheric forcing, so altered heat and freshwater fluxes shaping the mixed layer that is later subducted into the ocean interior will cause subsurface isopycnal changes (warming/freshening). On the other hand, the vertical displacement of density surfaces (which changes the properties at a given depth) can be caused either by changes in the rates of renewal of water masses or by dynamical changes affecting the density field structure. As water masses move further from their sources, the diffusive processes affecting their transformation contribute to blur the specific signatures acquired at the formation stages. Bindoff and McDougall (1994) developed a systematic methodology to characterize water mass changes, showing that observed changes along pressure surfaces can be approximately split into changes of properties along neutral density surfaces and changes due to the displacement of isopycnals through the vertical gradients of properties assumed constant over time.

$$\left.\frac{d\theta}{dt}\right|_p \simeq \left.\frac{d\theta}{dt}\right|_n - \left.\frac{dp}{dt}\right|_n \frac{\partial\theta}{\partial p} \tag{1}$$

$$\left.\frac{dS}{dt}\right|_p \simeq \left.\frac{dS}{dt}\right|_n - \left.\frac{dp}{dt}\right|_n \frac{\partial S}{\partial p}, \tag{2}$$

where $p$ and $n$ indicate, respectively, changes at isobars and isopycnals. The left-hand term is thus called the *isobaric change*, the first right-hand term the *isopycnal change* and the

**Table 2.** Potential density layers defining water masses with corresponding neutral densities ($\gamma^n$) and depth-averaged values of pressure ($\overline{P}$), potential temperature ($\overline{\theta}$) and salinity ($\overline{S}$).

| Water mass | Density (kg m$^{-3}$) | $\gamma^n$ (kg m$^{-3}$) | $\overline{P}$ (dbar) | $\overline{\theta}$ (°C) | $\overline{S}$ |
|---|---|---|---|---|---|
| ENACW | $27 < \sigma_\theta < 27.20$ | 27.06–27.26 | 298 | 12.15 | 35.70 |
| Sal min (core) | $\sigma_\theta \approx 27.2$ | 27.26 | 476 | 11.29 | 35.61 |
| MW | $31.85 < \sigma_1 < 32.25$ | 27.46–27.79 | 1003 | 10.06 | 35.85 |
| LSW (core) | $\sigma_2 \approx 36.88$ | 27.93 | 1765 | 4.63 | 35.13 |
| ENADW | $41.42 < \sigma_3 < 41.51$ | 28.02–28.100 | 3234 | 2.60 | 34.94 |
| LDW | $\sigma_4 \approx 45.86$ | 28.105 | 4500 | 2.08 | 34.90 |

second one the *heave term*. The vertical coordinate pressure $p$ is assimilated to the z-axis so Eqs. (1) and (2) may be written in compact notation as $\theta'_z \simeq \theta'_n - N'\theta_z$ and $S'_z \simeq S'_n - N'S_z$, where $N'$ is the change in height of the neutral surface and the primes indicate temporal change of the scalar quantities. We will apply this methodology in order to characterize the seasonal changes occurring in different water masses in the two regions.

Temporal changes are usually calculated by comparing properties between two cruises, regardless of the time-lag between them and lack of information about variability at shorter timescales. Since we have a true time series of hydrographical sections, we will consider changes referred to an overall average section instead of calculating changes between pairs of cruises. Therefore we will construct the series of anomalies of key properties (isopynal/isobaric changes and heave) with respect to the overall average section. From these series will be estimated the presence of seasonality and its amplitude.

## 4 Results

Vertical sections of salinity from the cruises series (Fig. 3) provide a first insight on the presence of a recurrent seasonal pattern in the structure of hydrographic fields, specially evident at the levels of Mediterranean water characterized by the salinity maximum (core c.a. $\sim 1000$ m). As expected, a saltier MW vein ($S \sim 36.2$) is tight against the slope year-round, but most occupations (though not all) show that this signature of MW on the slope tends to be stronger in summer, while in wintertime the MW core tends to be broader and displaced offshore, even concentrating in the surroundings of the Galicia Bank.

### 4.1 Seasonality amplitude and structure – slope and open ocean – isopycnal change vs. heave

The recurrence of structures in winter and in summer points to the existence of a seasonal cycle at depth. There are basically two methods for extracting the seasonal cycle from a time series (see for instance Chelton, 1982). The first consists

of carrying out a harmonic analysis of the data and reconstructing the seasonal cycle from the amplitudes and phases of the annual and higher order constituents (e.g. Bray, 1982). The second consists of computing the long-term mean value through the calendar year at the sampling interval of the time series (e.g. Thomson et al., 1985). The latter approach is generally preferred as it filters the slow-varying interannual variability and a seasonal cycle of arbitrary shape is not forced to accommodate to a reconstruction by few harmonics. On the other hand, this method may incorporate a strong bias if any specific section were strongly anomalous. In the present section we take the summer-average vs the winter-average of properties as the measure of their seasonal amplitude. Actually, our semiannual time series does not provide information to characterize the seasonality signature further. We will apply in Sect. 4.2 a simple harmonic analysis to key time series of the record in order to get a statistical measure of the robustness of the seasonality signal.

Figure 4 shows the seasonal changes of temperature, salinity, and density along the sections. Note that the anomalies are representing the summer minus winter condition, i.e. positive anomalies (red shades) indicate warmer, saltier or denser water along isobars or deeper isoneutrals during summertime. Here, the pattern previously inferred from Fig. 3 is clearly perceptible, with warmer and saltier waters from 1000 to 1750 m tight against the slope in summertime (from coast to about 10° W), versus colder and fresher from 11.5° W to 13.5° W over the Galicia Bank. This implies a warmer and saltier intermediate water broadening and spreading above the Galicia Bank in wintertime. Also clearly identifiable is the seasonal effect on the upper layers with warmer waters down to 100 dbar in summertime except over the shelf, where the effect of summer upwelling is notable. There is also a change in the density field structure with lighter surface waters (down to $\sim 100$ dbar) in summer than in winter, and denser water below; the near-surface ($\sim 100$ dbar) zero contour separating depths where the sign of the anomaly changes, shoals near the coast suggesting the presence of denser (and cooler) waters that are uplifted from the thermocline during summer upwelling. Changes in the density field (hence in pressure of density surfaces) accounts for the heave component of the isobaric changes in the ther-
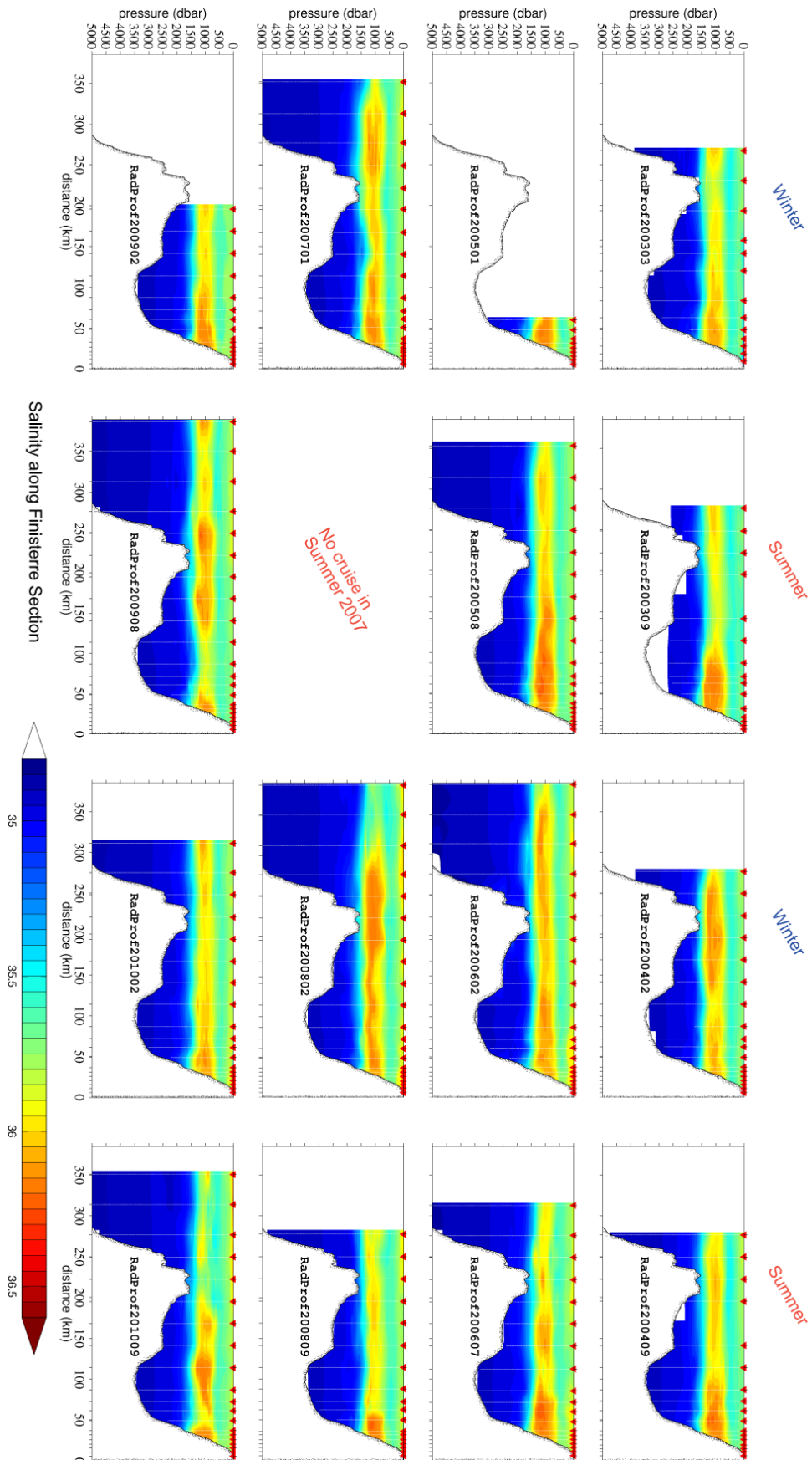
**Fig. 3.** Plate showing the salinity field structure for the 15 repetitions of the Finisterre section. Sections are showed in chronological order from left to right, with the first and third columns showing the winter cruises and the second and fourth columns showing the summer cruises, except that of summer 2007.

mohaline properties, implying changes in the geostrophic flow patterns in the ocean interior, as we will see later.

Right column of Fig. 4 shows the summer minus winter mean differences of $\theta$, $S$, and pressure of $\gamma^n$ surfaces, providing a graphical view of where properties on isopycnals change and where changes due to heave are of importance. Main results that can be drawn are (i) the strong isopycnal character of changes at the lower bound of Mediterranean waters, tight on the slope and west of the Galicia Bank. (ii) The high seasonal differences on isopycnal pressure levels above isopycnal 27.3 ($\sim 500$ dbar) all along the section, implying an isopycnal shoaling up to 50 dbar in summer with respect to the winter season. Such change is much pronounced on the slope and extends deeper. (iii) An apparent change in the structure of the density field around the Galicia Bank, with the sinking of isopycnals at its eastern flank in summertime at intermediate levels. This readjustment of the density field would imply an enhancement of geostrophic southwards flow in the passage from the Galicia Bank to the shelf during this season. Finally, (iv) there is an enhancement of a recirculation structure associated to the Galicia Bank in summertime.

It is interesting to get overall estimates of the amplitudes of annual cycles at depth. By inspection of Figs. 4a, b and even e, it looks rather like there are four distinct regions, one on the slope, one in the channel between the continent and the Galicia Bank, one east of the Bank and one west of it. These four regions appear to be linked to the recirculation system that develops in the surroundings of the Galicia Bank, which seems to yield a differentiated response to the seasonally varying background flows. We could easily apply the methodology of splitting isobaric changes that latter generate Fig. 5 to the four regions instead of the two proposed. The reason for keeping only two regions is that some of the subregions are narrow and involve very few stations. For instance, the anomaly at the eastern flank associated with warmer/saltier waters in summertime is confined to stations 15–17. Therefore, we prefer to keep a larger number of stations per region in order to get more reliable results from a statistical point of view, while keeping in mind that there are biases in the thermohaline seasonal signature in the outer and inner regions of the Bank due to its influence on the dynamics. Our approach assumes that, for the purpose of providing an overall view of the hydrographical variability of the outer ocean, the local anomalies caused by the Bank circulation should cancel each other out.

Thus, we consider separately the two regions (slope and outer ocean) and the methodology for splitting the changes, as in Eqs. (1) and (2), is applied at isopycnal levels from 27 to 28 kg m$^{-3}$. Then, amplitudes of the annual cycle for each of the terms in the decomposition relationship are obtained for every neutral density layer and seasonal anomalies are zonally averaged for each region.

A graphical view of the computation is shown in Fig. 5, which provides a continuous profile of seasonal amplitudes, while the numerical values are shown in Table 3 as anomalies at the pressure levels of key isopycnals.

The main results of the analysis can be summarized as follows:

– Waters just below the seasonal thermocline cool and freshen in summertime all along the section, with maximum changes at $\sim 200$ dbar ($\gamma^n \sim 27.1$). At the open ocean, maximum cooling/freshening values exceed $\sim 0.3$ °C and $\sim 0.02$, and this seasonality decays progressively down to $\sim 500$ dbar (the salinity minimum at the base of ENACW) where there is no signature at all. The process is driven mainly by heave. On the slope the behaviour is similar but the amplitudes are larger and seasonality extends deeper down the water column. In both areas there is a weaker (than heave) isopycnal warming/salting signature that cannot counteract the much greater cooling/freshening by heave.

– In the density range $\gamma^n \sim 27.3$–27.6 (500–900 dbar; upper MW) we observe cooling/freshening at the outer ocean (0.2 °C and 0.03) and salinification on the slope (0.05). Isopycnal change drives the cooling/freshening at the outer ocean and there is a slight salt increase centred at 27.45 (note that as this water layer is characterized by a weak or null thermal gradient – see Fig. 1d, e – it is not possible to achieve warming/cooling by heave). The salinity increase on the slope is caused by the strong uprising of isopycnals in this region (i.e. heave).

– The lower layer of MW down to the LSW (range $\gamma^n \sim 27.7$–27.95, 1100–1800 dbar) is the portion of the water column where the seasonal cycle is greatest. At the outer ocean there is strong cooling/freshening up to 0.5 °C / 0.1 , caused by the combination of isopycnal change and heave, the latter being dominant at 1400 dbar where the amplitude of seasonality peaks. On the contrary the warming and salting on the slope (up to 0.31 °C and 0.062 near 27.9) is strongly dominated by isopycnal change. Maximum values for the outer region may seem higher in Fig. 5 than those shown in Table 3; the reason is that Fig. 5 provides a continuous profile of seasonal amplitudes, while Table 3 extracts the values at the pressure levels of key isopycnals.

In summary, there exists a noticeable seasonality signature in the Finisterre section for the whole permanent thermocline, down to c.a. 2000 m. There is a notable asymmetry between the slope region and the outer ocean. ENACW properties oscillates by heave with stronger amplitude on the slope. Upper MW on the slope appears to be upraised in summertime, while at the outer ocean its signature weakens (cools and freshens without significant heave signature). The water layer corresponding to the lower MW exhibits the largest changes, with strong cooling/freshening at the outer ocean and warming/salting on the slope. Overall, it appears
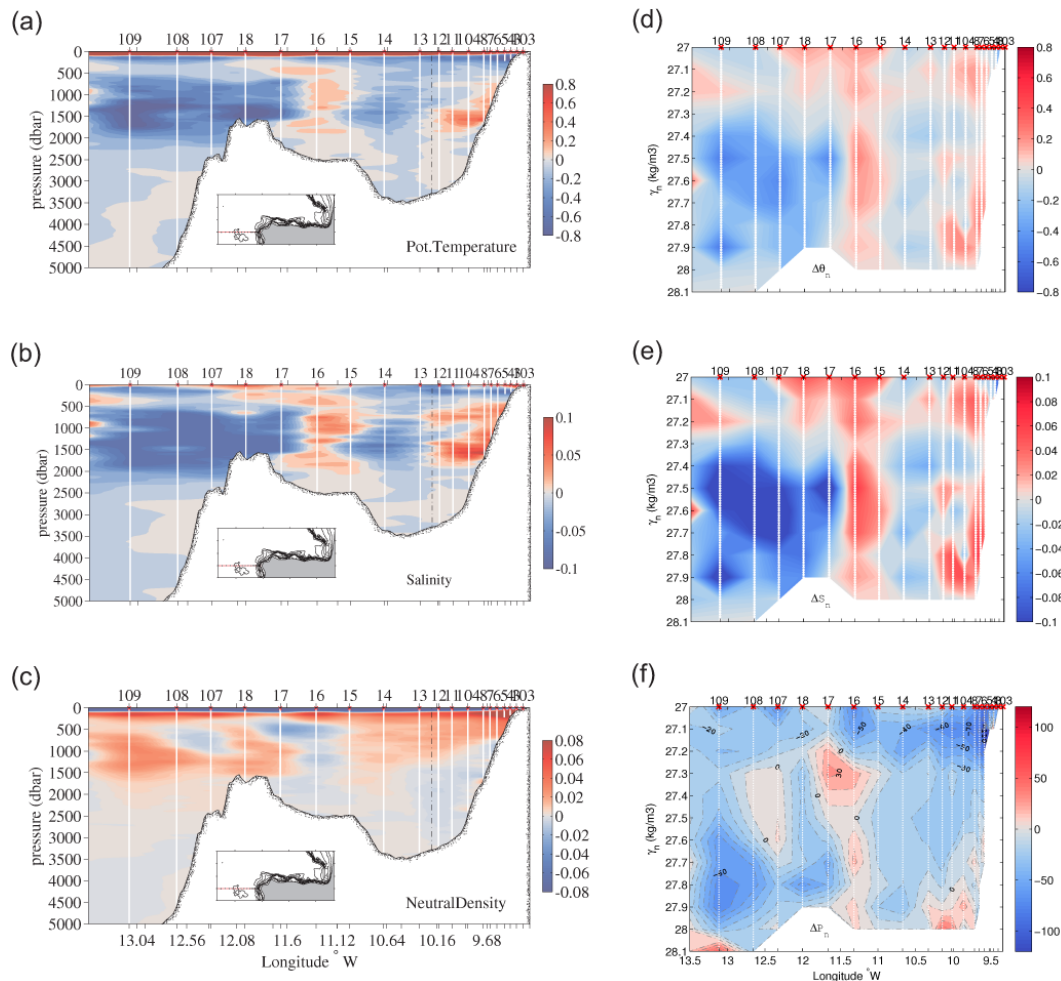
**Fig. 4.** Left column: summer–winter differences of **(a)** potential temperature, **(b)** salinity and **(c)** neutral density along isobaric surfaces. Right column: summer–winter differences of **(d)** potential temperature and **(e)** salinity along isoneutral surfaces with associated summer–winter differences of **(f)** isoneutrals pressure.

that MW during summertime gets tightly attached against the slope and uplifted, reinforcing there its thermohaline signature and losing its presence at the outer ocean. In wintertime the situation reverses, MW seems to detach from the slope and spreads out to the open ocean, even developing a secondary branch at, and west of, the Galician Bank.

## 4.2   Statistical significance of the seasonality signature

In this section we will check the robustness of the existence of seasonality from a statistical point of view. Testing for seasonality (or whatever periodic variation) in a time series relies in principle on spectral analysis, however, having a very limited number of observations and a signal with strong interannual variability (nonlinear trends) such seasonality testing is not straightforward. As previously noted, a convenient approach is to apply a simplified harmonic analysis determining the best fit of time series from hydrographical properties to

the functional form:

$$\psi(t) = a\cos(\omega t + \phi) = a_1\cos(\omega t) + a_2\sin(\omega t), \qquad (3)$$

where $\omega = 2\pi f$ is fixed to one year ($f = 1$, which is indeed the shortest solvable scale given the Nyquist frequency of our semiannual series). Then, it can be checked whether the amplitude coefficient is significant by means of a $t$ test. This approach was followed by Bray (1980) to determine seasonality of hydrographycal properties at intermediate levels in the Bay of Biscay, which is a very similar problem to ours, though her dataset consisted of 11 points along three years. Prior to attempt any harmonic analysis it is needed to remove the record mean and trends (linear or not) if relevant (e.g Emery and Thomson, 2001). This is indeed our case given that, as will be shown next, interannual variability is much larger than the apparent seasonality signal. Therefore, we treat our 8 yr time series of hydrographical properties subtracting firstly a two-degree polynomial (hence removing
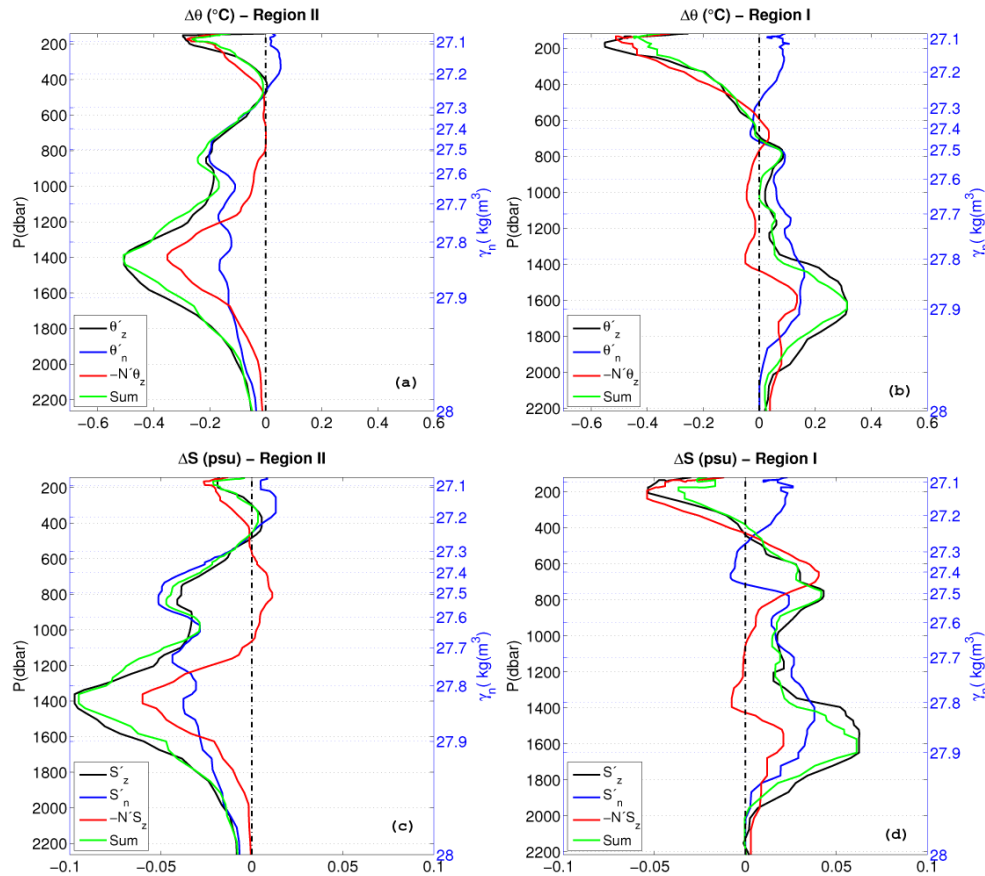
**Fig. 5.** Decomposition of $\theta$ (top) and $S$ (bottom) isobaric seasonal cycle following Eqs. (1) and (2). **(a)** and **(c)** are for the open ocean and **(b)** and **(d)** for the slope. Note that the decomposition is only approximate; the difference between the isobaric change (black line) and the sum (green line) of the isopycnal (blue line) and heave (red line) terms indicates the inaccuracy of the decomposition.

slowly varying patterns) to compute later the bestfit of Eq. (3) of the residual.

Figure 6 shows the bestfit of properties (salinity at isobars, pressure of isopycnals and salinity at isopycnals) at levels of selected neutral surfaces $\gamma^n = 27.4$ and $\gamma^n = 27.8$ for the slope region, where we have determined seasonality driven by heave and by isopycnal change respectively (Fig. 5). In accord with what is observed in the sections (Fig. 3), a see-saw pattern is intermittently present at portions of the time series. After the removal of the trend, the fitting results are significant for heave at 27.4 and for isopycnal change at 27.8. Anomalous years with opposed patterns also arise (e.g. summer 2009 again in agreement with Fig. 3). Figure 6 provides us an insight of the relative strength of the seasonality with respect to the interannual variability. Values of the estimated amplitude of seasonality represent roughly a 20 % of maximum variations or excursions along the whole time series of properties, interannual variability included (Fig. 6 and others not shown). In summary, this analysis reinforces the case for the existence of seasonality superimposed on the interannual variability of hydrographic properties at depth.

## 5 Discussion

As introduced in Sect. 2, the 43° N section (Finisterre section, Fig. 1) is located in the north-east limb of the North Atlantic subtropical gyre, an area of very weak circulation. Covering ~ 200 nm from the continental shelf to the open ocean and sampling the whole water column, its semiannual monitoring has provided the most detailed view of seasonality at all levels in the area to date.

Changes in the thermohaline properties at the sampling site may be caused by changes in the intrinsic properties of water masses and/or by changes in the circulation patterns (altering the water masses geographical distribution). It is however difficult to disentangle among them as the processes involved in the formation/transformation of water masses are intertwined with those altering the overall dynamics. As the water masses spread further from their sources towards the sampling site, it is more unlikely to discern a signature of shifts remotely imprinted on water properties, and even less any kind of seasonal swing. In the present Sect. we will discuss the observed seasonality signatures in our dataset in

**Table 3.** Decomposition of $\theta$ and S seasonal changes along isoneutral surfaces ($\gamma^n$) as isopycnal plus heave terms in the open ocean and shelf-slope region. Positive (negative) values indicate warmer/saltier (cooler/fresher) conditions in summertime. $P_n$ is the mean pressure of isoneutral $\gamma^n$ (see Fig. 5).

| $\gamma^n$ | $P_n$ (dbar) | $\theta'_z$ | $\theta'_n$ | $N'\theta_z$ | $\theta'_n - N'\theta_z$ | $S'_z$ | $S'_n$ | $N'S_z$ | $S'_n - N'S_z$ |
|---|---|---|---|---|---|---|---|---|---|
| Open ocean | | | | | | | | | |
| 27 | 142 | −0.09 | 0.02 | −0.19 | −0.16 | −0.017 | 0.007 | −0.013 | −0.004 |
| 27.1 | 187 | −0.27 | 0.01 | −0.15 | −0.16 | −0.018 | 0.001 | −0.016 | −0.016 |
| 27.2 | 367 | −0.01 | 0.04 | −0.06 | −0.01 | 0.005 | 0.010 | −0.006 | 0.004 |
| 27.3 | 558 | −0.05 | −0.04 | −0.01 | −0.05 | −0.011 | −0.012 | −0.000 | −0.011 |
| 27.4 | 677 | −0.13 | −0.14 | −0.00 | −0.14 | −0.025 | −0.036 | 0.007 | −0.028 |
| 27.5 | 791 | −0.19 | −0.19 | 0.00 | −0.22 | −0.038 | −0.050 | 0.011 | −0.044 |
| 27.6 | 927 | −0.18 | −0.13 | −0.04 | −0.18 | −0.032 | −0.035 | 0.004 | −0.031 |
| 27.7 | 1100 | −0.21 | −0.14 | −0.08 | −0.25 | −0.038 | −0.038 | −0.005 | −0.048 |
| 27.8 | 1314 | −0.43 | −0.11 | −0.29 | −0.42 | −0.084 | −0.029 | −0.048 | −0.080 |
| 27.9 | 1627 | −0.32 | −0.12 | −0.11 | −0.24 | −0.059 | −0.026 | −0.018 | −0.045 |
| 28 | 2264 | −0.05 | −0.03 | −0.01 | −0.04 | −0.008 | −0.006 | 0.000 | −0.007 |
| Shelf-slope | | | | | | | | | |
| 27 | 119 | −0.27 | 0.09 | −0.33 | −0.37 | −0.029 | 0.024 | −0.011 | −0.021 |
| 27.1 | 147 | −0.54 | 0.09 | −0.50 | −0.39 | −0.048 | 0.026 | −0.044 | −0.016 |
| 27.2 | 332 | −0.17 | 0.06 | −0.24 | −0.18 | −0.010 | 0.016 | −0.025 | −0.009 |
| 27.3 | 533 | −0.07 | −0.01 | −0.03 | −0.06 | 0.011 | −0.004 | 0.021 | 0.013 |
| 27.4 | 645 | −0.01 | −0.02 | 0.03 | −0.01 | 0.029 | −0.007 | 0.040 | 0.029 |
| 27.5 | 764 | 0.08 | 0.08 | 0.00 | 0.07 | 0.043 | 0.021 | 0.022 | 0.044 |
| 27.6 | 926 | 0.03 | 0.04 | −0.03 | 0.01 | 0.023 | 0.013 | 0.005 | 0.017 |
| 27.7 | 1120 | 0.04 | 0.09 | −0.01 | 0.06 | 0.020 | 0.026 | −0.001 | 0.021 |
| 27.8 | 1371 | 0.14 | 0.13 | −0.05 | 0.07 | 0.039 | 0.036 | −0.009 | 0.024 |
| 27.9 | 1649 | 0.31 | 0.15 | 0.10 | 0.31 | 0.062 | 0.033 | 0.017 | 0.062 |
| 28 | 2215 | 0.03 | 0.00 | 0.03 | 0.03 | 0.002 | 0.000 | 0.001 | 0.000 |
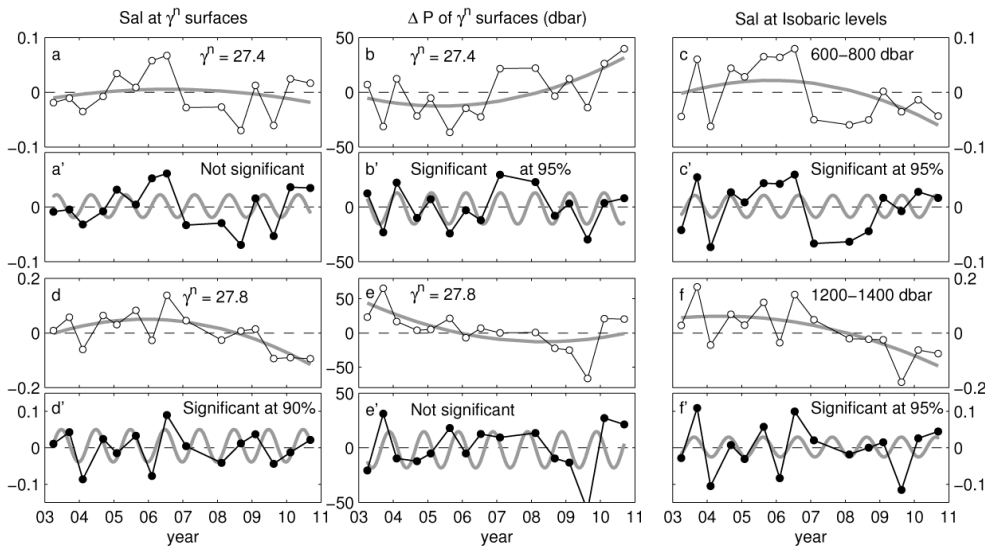


**Fig. 6.** Time series of **(a)**, **(d)** salinity anomaly at isopycnal levels $\gamma^n = 27.4$ and 27.8, **(b)**, **(e)** pressure (anomaly) at which these isopycnal levels lie, **(c)**, **(f)** salinity anomaly at isobaric levels 600–800 and 1200–1400 dbar, roughly corresponding to these isopycnals. A two-degree polynomial trend is computed for each series (thick gray). Prime versions of figures correspond to the simple harmonic analysis applied to the residual (time series minus trend, black dots) following Eq. (3).

the context of the known oceanographic processes that cause seasonality in the North Atlantic eastern boundary.

## 5.1 Large scale circulation: the subtropical gyre

Our first-glance overall view indicates a more intense presence of northern origin waters in summertime all along the open ocean region (colder and less saline waters at all depths). Such enhanced advection of subpolar waters during summer suggests large-scale fluctuations of the subtropical gyre (in position and/or strength).

Chidichimo et al. (2010) and Kanzow et al. (2010) studied the seasonality of transports at the subtropics, downstream of our sampling site, by means of time series measured by the RAPID-MOCHA array (26.5° N). They concluded that the major contribution of seasonality to the meridional overturning circulation is precisely the seasonality at the eastern boundary, characterized by a maximum southward transport in spring (between April–May). Other works studying the seasonal variability of the Canary Current indicate in agreement and enhancement of southwards flow in early spring and weakening and even reversal (poleward flows) in late summer–autumn at some levels (Machin et al., 2010; Mason et al., 2011). These changes in the subtropics are connected with seasonal variations in the shape of the subtropical gyre, which has a larger zonal (east–west) and smaller meridional (north–south) extents in summer than in winter (Stramma and Isemer, 1988). Upstream of our sampling site, the North Atlantic Current also appears to suffer seasonality in its transport. Specifically, Yaremchuk et al. (2001) studied the circulation of the upper 1000 m in the 40–55° N and 20–40° W region finding among other results that the outflow leaving the eastern side of their study box is maximum around April. Therefore, known seasonality of the subtropical gyre, both upstream (NAC eastwards leakage) and downstream (Canary Current system), points to an enhanced flow in spring and southward displacement of the overall subtropical gyre system in summer. These findings are consistent with the enhanced presence of northern waters in summertime at our sampling site.

The main forcing mechanism capable of altering the circulation of an oceanic basin is the seasonality in the wind stress and wind stress curl, which causes variability in Ekman transports (Stramma and Isemer, 1988) and rearrangements of the density field which trigger the generation of Rossby waves that later propagate westwards into the basin (Krauss and Wuebber, 1982). Actually, the subtropical gyre of the North Atlantic, particularly its eastern boundary, has been documented to be subject to large-scale seasonal variability in the wind stress curl (Bakun and Nelson, 1991, and Fig. 7).

Literature provides some clues in order to assess the role of propagating Rossby waves vs. Ekman transport in the observed seasonality at depth in our section, but a firm conclusion is difficult to achieve. Hirschi et al. (2007) studied the effect of seasonality in wind forcing on the meridional overturning circulation, stating that southwards of about 36° N the thermal wind contribution (variations of the density field) dominates the seasonal cycle while northwards of this latitude the major contribution is due to Ekman transport. In agreement, Osychny and Cornillon (2004) indicate from sea surface height (SSH) signatures that northwards of 41° N there is almost negligible energy at annual or shorter scales, being concentrated at periods longer than 1.5 yr. From these works, propagating Rossby waves at our 43° N section should not be expected to be the main contributor to the seasonality signatures at depth. On the other hand, Bray (1982) did attribute observational evidence of seasonal variability below the thermocline in the Bay of Biscay to the westward reflection of a seasonally wind-forced large-scale Rossby wave, and Friocourt et al. (2008) linked seasonal flow reversals of modelled slope currents to annual Rossby waves. As a matter of comparison, Fig. 8 provides wind stress curl annual anomalies obtained from the SCOW (scatterometer climatology of ocean winds) climatology (Risien and Chelton, 2008) at (i) the RAPID (Rapid Climate Change) /MOCHA (Meridional Overturning Circulation and Heat Transport Array) region at 26.5° N (where Kanzow et al. (2010) show that a wind stress curl forced Rossby wave model successfully accounts for the observed seasonality) and (ii) off Finisterre at 43° N. Wind stress curl anomaly that would trigger Rossby waves is 2–3 times weaker in our region.

## 5.2 Continental slope dynamics: upwelling, the Iberian Poleward Current and MW spreading

Shelf-slope dynamics at the western Iberian margin are subject to specific processes, some exhibiting strong seasonal character, that interact with the large-scale subtropical gyre seasonality. Northerly winds during the summer months cause widespread upwelling along the shelf (Wooster et al., 1976), while south-westerly winds in wintertime induce onshore Ekman transport. This upwelling/downwelling regime interacts with the slope dynamics characterized by the presence of the Iberian Poleward Current (IPC), a poleward flow driven by the meridional density gradient that carries warmer and saltier waters of southern origin (Haynes and Barton, 1990; Frouin et al., 1990; Pingree and Le Cann, 1990). The IPC is thought be a permanent feature although it reaches a maximum development in wintertime after the strengthening of the meridional density gradients in late fall and winter (Peliz et al., 2005), aided by downwelling favourable winds, which adds up to a fifth of the total transport (Frouin et al., 1990). On the contrary, during the summer the IPC is not observed at the sea surface and it is thought to be displaced offshore and to persist below the surface (Peliz et al., 2005; Ruiz-Villarreal et al., 2006).

The effect of the upwelling/downwelling cycle on the central waters is reflected in our dataset as enhanced cooling/freshening on the slope in summertime, down to 600 dbar, caused by heave (Fig. 5b, d). The minor warming
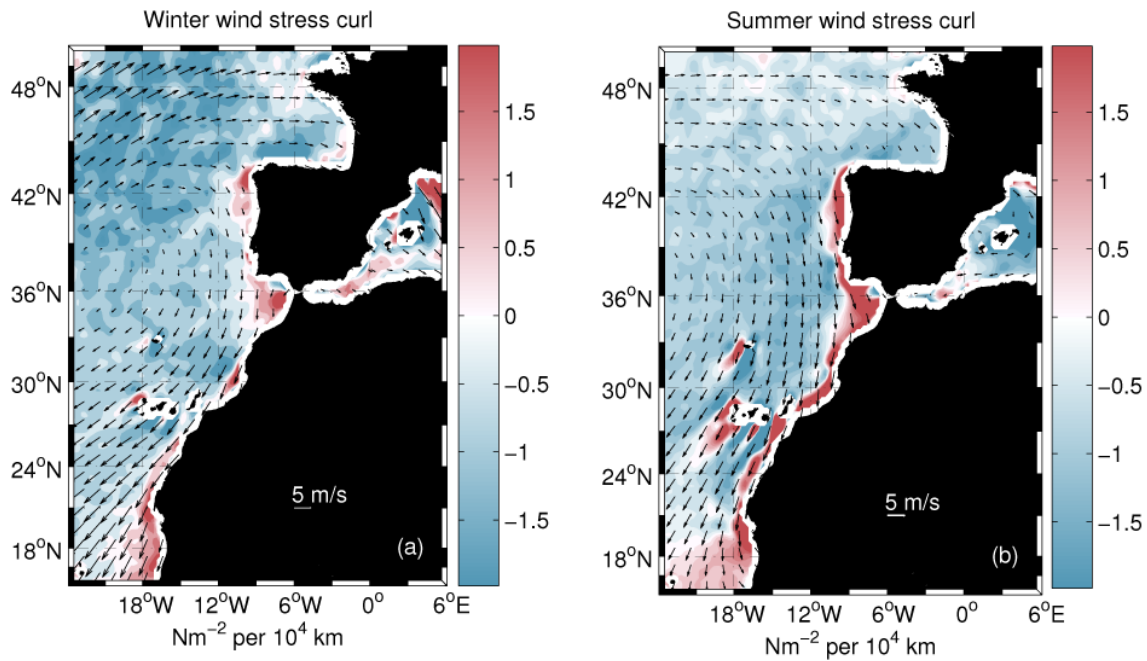
**Fig. 7. (a)** Winter and **(b)** summer wind stress curl in the North Atlantic. Arrows show the wind velocity field in both seasons

and salt increase at isopycnal levels on the slope in summertime is a striking signature (i.e. the 27.15 isoneutral is saltier and warmer in summertime but it lies much deeper). A rather speculative explanation for the presence of such central waters of southern origin on the slope in summertime may be linked to the presence of the deeper and offshore-displaced IPC pointed out by Peliz et al. (2005).

Below central waters, the seasonality at the level of MW appears a robust feature with contrasting character on the slope (more presence in summertime) and at the open ocean (more presence in wintertime). The MW spreading from the Gulf of Cádiz formation area has been widely studied (e.g. Iorga and Lozier, 1999a,b; Bower et al., 2002), but information about its seasonality is still scarce and relies on reduced datasets. Ambar et al. (1999) reported insights of seasonality of the MW spreading around the Portimao Canyon (off the southern coast of Portugal, 37° N) and off the north-west coast of Portugal at about 41° N, respectively from XBT lines and year-long current meter moorings between July 1993 and May 1994. Their main outcomes were a broader signature of MW in wintertime (i.e. more irregular and extending further offshore) and a cycle in temperature with notable offset: warming phases respectively at Portimao and 41° N from September–January and June–November (in agreement with our findings). Varela et al. (2005) also found a more intense MW signature in spring–summer on the slope at 42° N from a year-long weekly hydrostation between May 2000 and April 2001.

The IPC and the upwelling/downwelling cycle interacts with the dynamics of the Mediterranean water spreading at depth, and it has been proposed that poleward flows connect with the levels of MW (e.g. Torres and Barton, 2006). Garcia-Lafuente et al. (2008) provided indications of the coupling of MW and the upper slope dynamics while giving further insights of seasonality of the upper branch of the MW off north-western Iberia. From a 4-month record in the upwelling season, of two mooring lines located on the slope slightly northwards of 43° N, they concluded that during the settlement of a wind-induced upwelling the MW behaviour was consistent with a combination of a shoreward and upwards displacement of its core. Such result is in agreement with our observations of salt increase by heave down to 800 dbar on the slope. Moreover, we see that the along-slope vein gets strongly reinforced in summer down to its lower core with the presence of purer Mediterranean water (i.e. warmer and saltier on isopycnals) while the density structure remains. From a historical dataset of current meters, Huthnance et al. (2002) inferred flow reversals on the slope at ENACW and MW levels around February–March, an observation that also matches with the loss of presence of MW in winter on the slope.

Daniault et al. (1994) and Mazé et al. (1997) provided a larger-scale view of MW spreading along the Iberian margin and outer ocean, finding a bifurcation of the coastal trapped MW tongue south of the Galicia Bank at around 42° N. They proposed an anticyclonic circulation of MW around the Bank to later re-entry in the Iberia Basin, and suggested that the bifurcation may exhibit strong variability, though not necessarily seasonal. Their research was mostly supported by Bord-EST 3 cruise, taking place around May but "at a time when
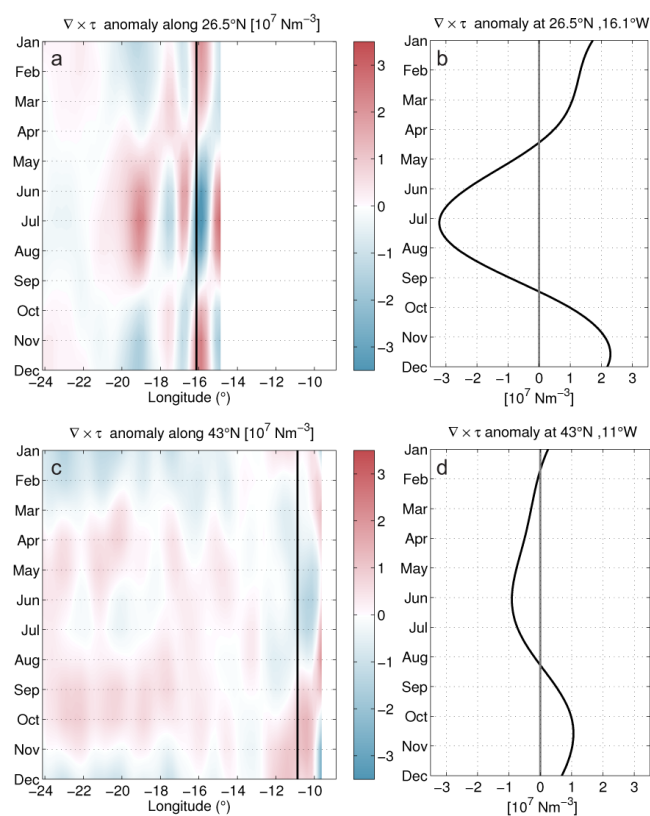
**Fig. 8.** Wind stress curl anomaly from SCOW climatology at **(a)** 26.5° N, **(c)** 43° N, and extracted for **(b)** 26.5° N, 16.125° W and **(d)** 43° N, 10.875° W

the near-surface winter regime was still dominant". Our results indicate that this pattern indeed corresponds to the typical hydrographical structure during wintertime. The diminished presence of MW in summertime at the outer region (colder and fresher at isopycnal levels) also implies a change in density structure (shoaling of isopycnals around $\gamma^n \sim 27.8$ making waters corresponding to the lower core of MW thinner). The pattern is consistent with the combination of the large-scale summer strengthening of the subtropical gyre and the reinforcement of MW along-slope vein.

## 5.3 Water masses formation at sources

### 5.3.1 ENACW mode water

Circulation and thermohaline properties of the central water east of the mid-Atlantic Ridge between 39° N and 54° N were analysed by Pollard et al. (1996) who observed that most of the transport associated with the North Atlantic Current (NAC) west of 20° W flows northwards (20 Sv) but that 10 Sv recirculate anticyclonically towards the west of the Iberian Peninsula, within the region south of the North Atlantic Current. Mazé et al. (1997) determined that the eastward flow

towards the Iberian Margin at 12.5° W was of the order of 2 Sv from 38° N to 43° N.

The majority of ENACW water is formed by deep winter convection in a region north of 45° N from where it is subducted and advected southwards, being the main ventilation region of mode waters in the North Atlantic. The annual renewal of these mode waters was studied in detail from hydrography data and air–sea flux budgets (e.g. Paillet and Arhan, 1996a,b), the region at the Finisterre section being a frontal zone marked by an abrupt meridional shoaling of winter mixed layers (between 40° N and 45° N). Gaillard et al. (2005) conducted specific studies west of the Finisterre section (POMME–Multidisciplinary Meso Scale Ocean Program–area) finding a relevant contribution of the mesoscale activity in the net subduction rate of mode waters.

Pérez et al. (2000) described that the thermohaline properties of regional ENACW exhibit strong decadal variability related to large-scale climatic patterns affecting air–sea fluxes variability at the areas of formation. On the contrary, at seasonal timescales Pérez et al. (1995) found "a gradual increase of temperature and salinity from spring to late autumn" both at the open ocean and on the shelf without any insights of seasonality of salinity at ENACW isopycnal level. In agreement with their results, we observe colder and fresher waters in summertime due to the uplifting of ENACW isopycnal levels. Such a cycle can be associated, besides the dynamic response to the upwelling cycle, with a greater thickness of the well-mixed new mode waters in spring, just after the end of entrainment phase and during the subduction period (Marshall et al., 1993).

### 5.3.2 MOW

There is even evidence of seasonality of MW right at its origin. Recent observations of the Mediterranean outflow water in the Strait of Gibraltar (Garcia-Lafuente et al., 2007) showed the existence of a seasonal cycle with warmer and lighter water leaving the Mediterranean Sea in winter, and cooler and denser waters in spring and summer (exhibiting also a maximum in transport) with amplitudes $\Delta T \sim 0.05\,°C$ and $\Delta \sigma \sim 0.015\,\text{kg}\,\text{m}^{-3}$. Fusco et al. (2008) reported seasonality in the Gulf of Cádiz with a salinity maximum around May–June, apparently in agreement with the maximum outflow around spring. Following the work of Daniault et al. (1994), the amount of pure Mediterranean outflow waters present in the MW vein around Finisterre is about a fifth ($\sim 20\,\%$, see their Fig. 14). Therefore seasonality of MW at source cannot be the cause of the actual observed changes but only of a minor fraction.

## 5.4 Results from circulation models

Some modelling exercises within the area have focused on seasonality either at the boundary or offshore, and from surface to mid-depths, providing a non-homogeneous set of out-
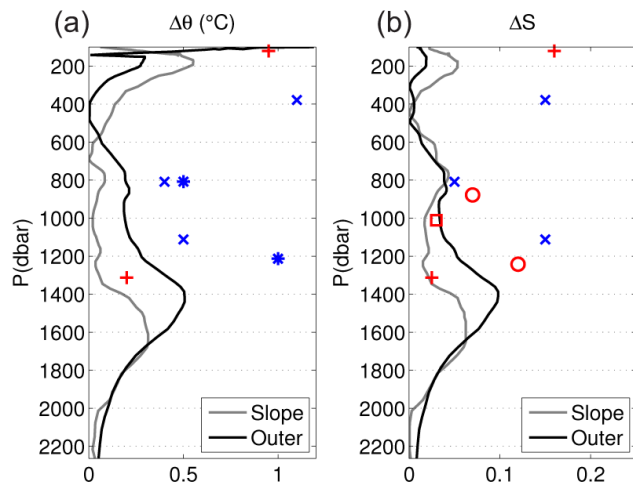
**Fig. 9. (a)** Potential temperature and **(b)** salinity isobaric changes in the slope (grey line) and outer ocean (black line) superimposed by seasonal anomalies found by Chidichimo et al. (2010) (+), Machin et al. (2010) (∘), Ambar et al. (1999) (∗), Varela et al. (2005) (×) and Bray (1982) (□).

comes. For example, a large-scale model of MW spreading used by Filyushkin et al. (2008) indicated pronounced seasonality in the transport through the Strait of Gibraltar but did not find a noticeable seasonal signature in salinity distributions of MW across the North Atlantic. A more regional model focused on the western Iberian margin provided by Coelho et al. (2002) succeeded in reproducing the general pattern and seasonal variations of upper circulation, including upwelling during the summer, a winter surface poleward current over the shelf and a permanent year-round undercurrent transporting MW along the Portuguese and Spanish slopes. The model was also able to account for notable offshore export of MW at 41–42° N, in agreement with observations, but it did not find a clear difference between winter and summer at MW levels.

Among modelling efforts that suggest notable seasonality at depth, stands the work of Friocourt et al. (2007). This study, supported by a regional model including western Iberia and the Bay of Biscay, simulates a strong baroclinic slope current at 42° N with a complex structure having cores at different levels and seasonal flow reversals at all depths. Salinity distribution in the core of MW indicates the presence of two flows: a narrow jet trapped on the slope, and a wider tongue flowing intermittently north-westwards toward the Galicia Bank. The position of the offshore MW tongue varies throughout the year, remaining in the vicinity of the slope from July to October and starting to move offshore around November, while the slope jet weakens and even reverses (i.e. flows equatorward) from November to January. Friocourt et al. (2008) elaborated further on the seasonality of the slope current showing that reversals of the deeper slope currents are at least partly forced by seasonal changes in the

flow upstream of the slope-current system. Slater (2003) provided, from the large-scale OCCAM (Ocean Circulation and Climate Advanced Modelling) model, a pretty similar outcome showing boundary flow at MW depths directed northward year-round but displacing offshore in winter when a southward flow on the slope develops below 300 m. Both descriptions agree with our results, although we can not infer from our dataset whether the along slope MW vein comes to reverse in winter or simply weakens.

## 5.5 Quantitative comparison of seasonality with other regions of the north-east Atlantic Ocean

As pointed out in the preceding discussion sections, there are many different dynamical processes that may imprint seasonality on to the deep ocean. However, many of the reviewed works only provide qualitative insights of seasonality or quantitative fluctuations of properties in a limited time frame, and rarely estimates of seasonal amplitude. All the available data about seasonal estimates collected in the reviewed literature have been joined with the seasonal isobaric changes found in our section, both in the slope and outer region (black lines in Fig. 5) in order to make a quantitative comparison between them (see Fig. 9). Chidichimo et al. (2010) estimated the seasonal amplitude in potential temperature and salinity from the EBH(eastern boundary)–RAPID mooring array (4 yr continuous record) at the subtropical North Atlantic eastern boundary along 26.5° N, finding anomalies of 0.95°C, 0.16 at 120 m and 0.2°C, 0.025 at 1300 dbar. These values are in accord with our temperature seasonal anomalies at the outer upper ocean (see Fig. 9a) and temperature and salinity anomalies of intermediate layers in the shelf-slope region (0.14°C and 0.03 along 27.8). A little to the north, seasonality estimated by Machin et al. (2010) from the 9 yr continuous record of EBC4 mooring at 28°46′ N, 13°28′ W in the Lanzarote Passage (Canary Basin), was ∼ 0.07 at 870 m and ∼ 0.12 at 1230 m in salinity from July–October and from November–December, when maximum salinity was found in both levels. Off the northern coast of Portugal, from a specific mooring at 41° N, 9°44′ W, Ambar et al. (1999) also observed a shift from summer to winter of 0.5°C at 800 m and 1°C at 1000 m, between July 1993 and May 1994. In the Galician shelf/slope, a shift was also observed from summer to winter in a year-long series, from May 2000 to April 2001, of weekly hydrographical profiles at fixed location 42.13° N, 9.5° W by Varela et al. (2005): they found seasonal shifts in temperature and salinity of about 1.1°C and 0.15 at ENACW$_{sp}$ levels (300–450 m), 0.4°C and 0.05 at the upper MW (∼ 800 m) and 0.5°C and 0.15 in the lower MW (∼ 1100 m). In these cases, seasonal estimates are, in general, higher than those encountered in our section. Bray (1982) also estimated a seasonal amplitude of 0.03 in salinity at ∼ 1000 m, from a series of 11 cruises over 3 yr in the Bay of Biscay area (2–20°W, 42–52°N), in concordance with our results (∼ 0.02–0.03 along 27.6–27.7 between 900–
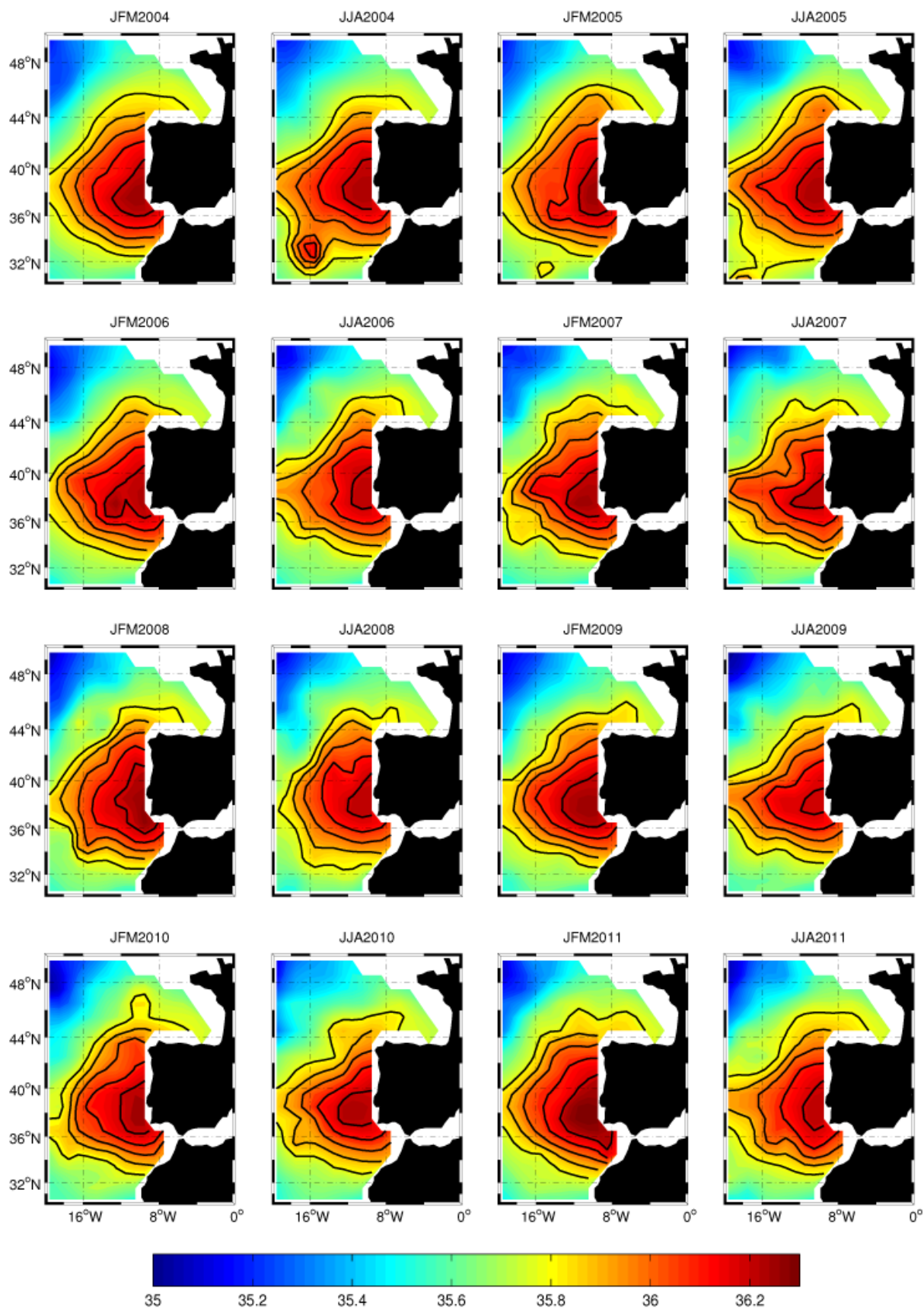
**Fig. 10.** Winter (JFM) and summer (JJA) salinity fields at 1000–1250 dbar level from Argo floats for the period 2004–2011. Black contours are plotted from 35.8 to 36.2 every 0.1.
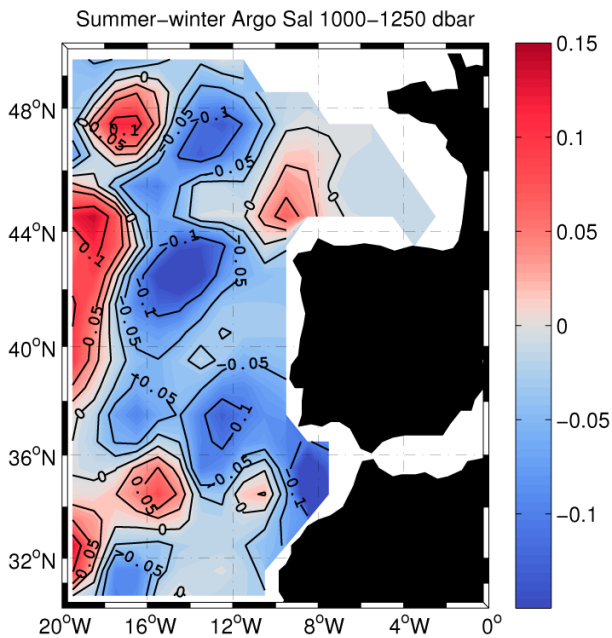
**Fig. 11.** Summer (JJA)–winter (JFM) average salinity field at 1000-1250 dbar level from Argo floats for the period 2004–2011
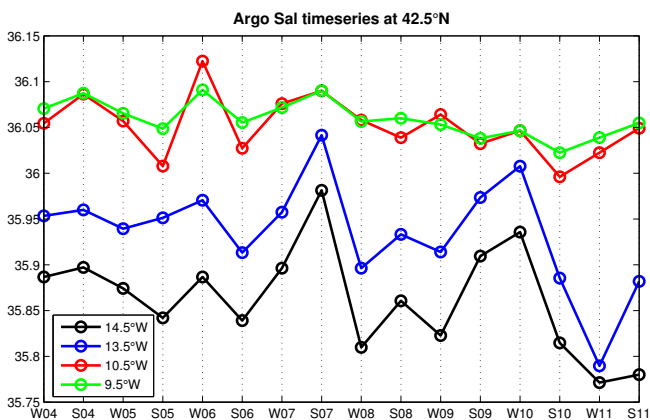


**Fig. 12.** Time series of the salinity field along the 42.5° N section from the interpolated field at 1000–1250 dbar level from Argo floats for the period 2004–2011, at different locations in the slope (9.5° W and 10.5° W) and the outer ocean region west of the Galicia Bank (13.5° W and 14.5° W)

1100 dbar). Note that red points in Fig. 9 represent observations spanning several years (from 3 to 9 yr), while those in blue are based on 1 yr sampling. We would like to highlight here the importance of establishing continuous and long time series of ocean properties in order to get a statistically significant seasonal cycle.

### 5.6  Capability of Argo floats to resolve seasonality in Finisterre

It is interesting to determine whether the spatio-temporal coverage of the Argo fleet is enough to resolve the seasonal signature as our in situ dataset does. We used the data viewer interface provided by the Argo website (http://www.argo.ucsd.edu/index.html) to retrieve the winter (January/February/March) and summer (June/July/August) salinity maps averaged for the Mediterranean water influence levels (1000–1250 dbar) in the region 30–50°N, 0–20°W (Fig 10). It appears difficult to evidence a recurrent seasonal pattern from such horizontal sections. The inspection of the available profiles (figures not shown) that support each of these interpolated field evidences that there may be large areas without profiles, specially the slope region, which is strongly undersampled (currents are stronger at these areas so floats are quickly advected). Nevertheless, we have computed the summer minus winter anomaly map (Fig. 11). The overall general view indicates less MW content in the open ocean of western Iberia in summertime (out to 16° W), which is consistent with our results from the section, and a higher MW content patch at the northwestern corner, which could be interpreted in a very speculative manner as a signature of enhanced northwards MW slope flow in summertime. However, the patchy character of the fields raises suspicions on its representativeness and the increase of MW in summertime west of 16°W seems quite odd. Fig. 12 provides the time series from interpolated fields at some locations in the eastern boundary along 42.5° N. Though there are periods when there appears to be a seasonally oscillating behavior, the time series yields much less clear signs of seasonality than the time series derived from the hydrographical section do. In summary, we do not feel that we can draw firm conclusions about seasonality of the western Iberian margin hydrography from the Argo buoys, especially at the slope. Their coverage is not enough to capture the seasonal changes in the whole water column; the continuous repetition of the hydrographical section is becoming worthwhile for the study of the regional deep oceanography in the western Iberia at seasonal timescales.

## 6  Conclusions

Hydrographical properties of a zonal section $\sim 200$ nm off Cape Finisterre (43° N, 009–014° W) have been sampled for the period 2003–2010 by means of two cruises per year (summer/winter). The sampling has revealed that there exists a noticeable seasonal signature in this part of the eastern boundary of the North Atlantic down to 2000 dbar. The magnitude of seasonality is roughly 20 % of the interannual variability observed for the overall period, reaching values up to 0.5 °C, 0.04 in salinity just below the maximum extent of winter mixing (c.a. 200 dbar), and 0.4 °C and 0.08

in salinity at around 1400 dbar, within the lower bounds of Mediterranean water.

The spatial structure of the seasonality shows a strong contrast between the near-slope area and the outer ocean. The most remarkable and novel finding is the behaviour of the Mediterranean water vein that gets attached and reinforced along the slope in summer and spreads offshore in wintertime. The observed pattern confirms, from a much larger dataset, some dynamical aspects regarding the Iberian margin seasonality and MW spreading that had been previously inferred from quite reduced datasets. Among them we can highlight the shoreward and upwards displacement of slope MW as a response to the seasonal upwelling and the appearance of a secondary branch of MW around the Galicia Bank, a feature that appears to be typical of the winter regime. The results have been discussed in terms of the seasonality of large-scale and continental slope processes and a brief review of modelling efforts regarding seasonality at the area has been made, showing that key features, reproduced by some of them as the winter flow reversal at MW levels on the slope, are consistent with our observations. The time series of in situ data provided here become a valuable tool for evaluating circulation models at regional or oceanic scales. The seasonality in the area must be taken into account when analysing specific hydrographical observations or long-term series.

# References

Ambar, I., Armi, L., Bower, A., and Ferreira, T.: Some aspects of time variability of the Mediterranean Water off south Portugal, Deep-Sea Research. I, 46, 1109–1136, doi:10.1016/S0967-0637(99)00006-0, 1999.

Bakun, A. and Nelson, C. S.: The Seasonal Cycle of Wind-Stress Curl in Subtropical Eastern Boundary Current Regions, J. Phys. Oceanogr., 21, 1815–1834, doi:10.1175/1520-0485(1991)021, 1991.

Bindoff, N. L. and McDougall, T. J.: Diagnosing climate change and ocean ventilation using hydrographic data, J. Phys. Oceanogr., 24, 1137–1152, doi:10.1175/1520-0485(1994)024, 1994.

Bower, A. S., Serra, N., and Ambar, I.: Structure of the Mediterranean Undercurrent and Mediterranean Water spreading around

the southwestern Iberian Peninsula, J. Geophys. Res., 107, 3161, doi:10.1029/2001JC001007, 2002.

Bray, N. A.: Seasonal variability in the intermediate waters of the Eastern North Atlantic, Ph.D. thesis, Woods Hole Oceanographic Institution, 1980.

Bray, N. A.: Seasonal variability in the Intermediate Waters of the eastern North Atlantic, J. Phys. Oceanogr., 12, 972–983, doi:10.1175/1520-0485(1982)012¡0972:SVITIW¿2.0.CO;2, 1982.

Chelton, D. B.: Statistical Reliability and the Seasonal Cycle – Comments on Bottom Pressure Measurements Across the Antarctic Circumpolar Current and Their Relation to the Wind, Deep-Sea Res., 29, 1381–1388, doi:10.1016/0198-0149(82)90016-4, 1982.

Chidichimo, M., Kanzow, T., Cunningham, S., Johns, W., and Marotzke, J.: The contribution of eastern-boundary density variations to the Atlantic meridional overturning circulation at 26.5 degrees N, Ocean Sci., 6, 475–490, doi:10.5194/os-6-475-2010, 2010.

Coelho, H. S., Neves, R. J. J., White, M., Leitao, P. C., and Santos, A. J.: A model for ocean circulation on the Iberian coast, J. Mar. Sys., 32, 153–179, doi:10.1016/S0924-7963(02)00032-5, 2002.

Daniault, J. P., Mazé, J. P., and Arhan, M.: Circulation and mixing of Mediterranean Water west of the Iberian Peninsula, Deep-Sea Res. I, 41, 1685–1714, doi:10.1016/0967-0637(94)90068-X, 1994.

Emery, W. J. and Thomson, R. E.: Data Analysis Methods in Physical Oceanography, Elsevier, 2001.

Filyushkin, B. N., Moshonkin, S. N., and Kozhelupova, N. G.: Seasonal evolution of the mediterranean water propagation in the north Atlantic, Oceanology, 48, 771–779, doi:10.1134/S0001437008060027, 2008.

Fiúza, A. F. G., Hamann, M., Ambar, I., del Río, G. D., González, N., and Cabanas, J. M.: Water masses and their circulation off western Iberia during May 1993, Deep-Sea Res. I, 45, 1127–1160, doi:10.1016/S0967-0637(98)00008-9, 1998.

Friocourt, Y., Levier, B., Speich, S., Blanke, B., and Drijfhout, S. S.: A regional numerical ocean model of the circulation in the Bay of Biscay, J. Geophys. Res., 112, C09008, doi:10.1029/2006JC003935, 2007.

Friocourt, Y., Blanke, B., Drijfhout, S., and Speich, S.: On the Dynamics of the Slope Current System along the West European Margin, Part II: Analytical Calculations and Numerical Simulations with Seasonal Forcing, J. Phys. Oceanogr., 38, 2619–2638, doi:10.1175/2008JPO3745.1, 2008.

Frouin, R., Fiúza, A. F. G., Ambar, I., and Boyd, T. J.: Observations of a poleward surface current off the coasts of Portugal and Spain during winter, J. Geophys. Res., 95, 679–691, doi:10.1029/JC095iC01p00679, 1990.

Fusco, G., Artale, V., Cotroneo, Y., and Sannino, G.: Thermohaline variability of Mediterranean Water in the Gulf of Cadiz, 1948–1999, Deep-Sea Res. I, 55, 1624–1638, doi:10.1016/j.dsr.2008.07.009, 2008.

Gaillard, F., Mercier, H., and Kermabon, C.: A synthesis of the POMME physical data set: One year monitoring of the upper layer, J. Geophys. Res., 110, C07S07, doi:10.1029/2004JC002764, 2005.

Garcia-Lafuente, J., Sanchez-Roman, A., Diaz-del Rio, G., Sannino, G., and Sanchez-Garrido, J. C.: Recent observa-

tions of seasonal variability of the Mediterranean outflow in the Strait of Gibraltar, J. Geophys. Res., 112, C10005, doi:10.1029/2006JC003992, 2007.

Garcia-Lafuente, J., Sanchez-Garrido, J. C., Diaz-del Rio, G., Criado-Aldeanueva, F., Marcote, D., and Sanchez-Roman, A.: Low-frequency variability of the Mediterranean undercurrent off Galicia, northwestern Iberian Peninsula, J. Mar. Sys., 74, 351–363, doi:10.1016/j.jmarsys.2008.02.007, 2008.

Haynes, R. and Barton, E. D.: A poleward flow along the Atlantic coast of the Iberian Peninsula, J. Geophys. Res., 95, 11425–11441, doi:10.1029/JC095iC07p11425, 1990.

Hirschi, J. J. M., Killworth, P. D., and Blundell, J. R.: Subannual, seasonal, and interannual variability of the North Atlantic meridional overturning circulation, J. Phys. Oceanogr., 37, 1246–1265, doi:10.1175/JPO3049.1, 2007.

Huthnance, J. M., van Aken, H. M., White, M., Barton, E. D., Le Cann, B., Coelho, E. F., Fanjul, E. A., Miller, P., and Vitorino, J.: Ocean margin exchange - water flux estimates, J. Mar. Sys., 32, 107–137, doi:10.1016/S0924-7963(02)00034-9, 2002.

Iorga, M. C. and Lozier, M. S.: Signatures of the Mediterranean outflow from a North Atlantic climatology 1, Salinity and density fields, J. Geophys. Res., 104, 25 985–26 009, doi:10.1029/1999JC900115, 1999a.

Iorga, M. C. and Lozier, M. S.: Signatures of the Mediterranean outflow from a North Atlantic climatology 2, Diagnostic velocity fields, J. Geophys. Res., 104, 26 011–26 029, doi:10.1029/1999JC900204, 1999b.

Jackett, D. R. and McDougall, T. J.: A neutral density variable for the World's Oceans, J. Phys. Oceanogr., 27, 237–263, doi:10.1175/1520-0485(1997)027¡0237:ANDVFT¿2.0.CO;2, 1997.

Kanzow, T., Cunningham, S. A., Johns, W. E., Hirschi, J. J. M., Marotzke, J., Baringer, M. O., Meinen, C. S., Chidichimo, M. P., Atkinson, C., Beal, L. M., Bryden, H. L., and Collins, J.: Seasonal Variability of the Atlantic Meridional Overturning Circulation at 26.5° N, J. Clim., 23, 5678–5698, doi:10.1175/2010JCLI3389.1, 2010.

Krauss, W. and Wuebber, C.: Response of the North-Atlantic to Annual Wind Variations Along the Eastern Coast, Deep-Sea Res. A, 29, 851–868, doi:10.1016/0198-0149(82)90050-4, 1982.

Machin, F., Pelegri, J. L., Fraile-Nuez, E., Velez-Belchi, P., Lopez-Laatzen, F., and Hernandez-Guerra, A.: Seasonal Flow Reversals of Intermediate Waters in the Canary Current System East of the Canary Islands, J. Phys. Oceanogr., 40, 1902–1909, doi:10.1175/2010JPO4320.1, 2010.

Marshall, J. C., Nurser, A. J. G., and Williams, R. G.: Inferring the Subduction Rate and Period Over the North-Atlantic, J. Phys. Oceanogr., 23, 1315–1329, doi:10.1175/1520-0485(1993)023¡1315:ITSRAP¿2.0.CO;2, 1993.

Mason, E., Colas, F., Molemaker, J., Shchepetkin, A. F., Troupin, C., McWilliams, J. C., and Sangra, P.: Seasonal variability of the Canary Current: A numerical study, J. Geophys. Res., 116, C06001, doi:10.1029/2010JC006665, 2011.

Mazé, J. P., Arhan, M., and Mercier, H.: Volume budget of the eastern boundary layer off the Iberian Peninsula, Deep-Sea Res. I, 44, 1543–1574, doi:10.1016/S0967-0637(97)00038-1, 1997.

Memery, L., Reverdin, G., Paillet, J., and Oschlies, A.: Introduction to the POMME special section: Thermocline ventilation and biogeochemical tracer distribution in the northeast Atlantic Ocean and impact of mesoscale dynamics, J. Geophys. Res., 110, C07S01, doi:10.1029/2005JC002976, 2005.

Osychny, V. and Cornillon, P.: Properties of Rossby waves in the North Atlantic estimated from satellite data, J. Phys. Oceanogr., 34, 61–76, doi:10.1175/1520-0485(2004)034¡0061:PORWIT¿2.0.CO;2, 2004.

Paillet, J. and Arhan, M.: Oceanic ventilation in the eastern North Atlantic, J. Phys. Oceanogr., 26, 2036–2052, doi:10.1175/1520-0485(1996)026¡2036:OVITEN¿2.0.CO;2, 1996a.

Paillet, J. and Arhan, M.: Shallow pycnoclines and mode water subduction in the eastern North Atlantic, J. Phys. Oceanogr., 26, 96–114, doi:10.1175/1520-0485(1996)026¡0096:SPAMWS¿2.0.CO;2, 1996b.

Paillet, J. and Mercier, H.: An inverse model of the eastern North Atlantic general circulation and thermocline ventilation, Deep-Sea Res. I, 44, 1293–1328, doi:10.1016/S0967-0637(97)00019-8, 1997.

Peliz, A., Dubert, J., Santos, A. M. P., Oliveira, P. B., and Le Cann, B.: Winter upper ocean circulation in the Western Iberian Basin – fronts, eddies and poleward flows: an overview, Deep-Sea Res. I, 52, 621–646, doi:10.1016/j.dsr.2004.11.005, 2005.

Pérez, F. F., Ríos, A. F., King, B. A., and Pollard, R. T.: Decadal changes of the theta -S relationship of the eastern North Atlantic Central Water, Deep-Sea Res. I, 42, 1849–1864, doi:10.1016/0967-0637(95)00091-7, 1995.

Pérez, F. F., Pollard, R. T., Read, J. F., Valencia, V., Cabanas, J. M., and Ríos, A. F.: Climatological coupling of the thermohaline decadal changes in Central Water of the Eastern North Atlantic, Sci. Mar., 64, 347–353, doi:10.3989/scimar.2000.64n3347, 2000.

Pingree, R. D.: Component of Labrador Sea-Water in Bay-Of-Biscay, Limnol. Oceanogr., 18, 711–718, doi:10.4319/lo.1973.18.5.0711, 1973.

Pingree, R. D. and Le Cann, B.: Structure, strength and seasonality of the slope currents in the Bay of Biscay region, J. Mar. Biol. Assoc. U. K., 70, 857–885, doi:10.1017/S0025315400059117, 1990.

Pollard, R. T. and Pu, S.: Structure and circulation of the upper Atlantic Ocean northeast of the Azores, Prog. Oceanogr., 14, 443–462, doi:10.1016/0079-6611(85)90022-9, 1985.

Pollard, R. T., Griffiths, M. J., Cunningham, S. A., Read, J. F., Pérez, F. F., and Ríos, A. F.: Vivaldi 1991 – a study of the formation, circulation and ventilation of eastern North Atlantic Central Water, Prog. Oceanogr., 37, 167–192, doi:10.1016/S0079-6611(96)00008-0, 1996.

Risien, C. M. and Chelton, D. B.: A Global Climatology of Surface Wind and Wind Stress Fields from Eight Years of QuikSCAT Scatterometer Data, J. Phys. Oceanogr., 38, 2379–2413, doi:10.1175/2008JPO3881.1, 2008.

Ruiz-Villarreal, M., González-Pola, C., Díaz del Río, G., Lavín, A., Otero, P., Piedracoba, S., and Cabanas, J. M.: Oceanographic conditions in North and Northwest Iberia and their influence on the Prestige oil spill, Mar. Pollut. Bull., 53, 220–238, doi:10.1016/j.marpolbul.2006.03.011, 2006.

Slater, D.: The transport of Mediterranean Water in the North Atlantic Ocean, Ph.D. thesis, University of Southampton, UK, 2003.

Solomon, S., Qin, D., Manning, M., Marquis, M., Averyt, K., Tignor, M. M. B., Miller, H. L., and Chen, Z., eds.: Climate Change

2007 - The Physical Science Basis: Working Group I Contribution to the Fourth Assessment Report of the IPCC (Climate Change 2007), Cambridge University Press, Cambridge, 2007.

Stramma, L. and Isemer, H. J.: Seasonal Variability of Meridional Temperature Fluxes in the Eastern North-Atlantic Ocean, J. Mar. Res., 46, 281–299, doi:10.1357/002224088785113577, 1988.

Thomson, R. E., Tabata, S., and Ramsdem, D.: Comparison of sea level variability on the Caribbean and the Pacific coasts and the Panama canal, in: Time series of ocean measurements, vol. 2 of IOC Technical Series, UNESCO, 33–37, 1985.

Torres, R. and Barton, E. D.: Onset and development of the Iberian poleward flow along the Galician coast, Cont. Shelf. Res., 26, 1134–1153, doi:10.1016/j.csr.2006.03.009, 2006.

van Aken, H. M.: The hydrography of the mid-latitude Northeast Atlantic Ocean. I: The deep water masses, Deep-Sea Res. I, 47, 757–788, doi:10.1016/S0967-0637(99)00092-8, 2000a.

van Aken, H. M.: The hydrography of the mid-latitude Northeast Atlantic Ocean – Part II: The intermediate water masses, Deep-Sea Res. I, 47, 789–824, doi:10.1016/S0967-0637(99)00112-0, 2000b.

van Aken, H. M.: The hydrography of the mid-latitude Northeast Atlantic Ocean – Part III: The subducted thermocline water mass, Deep-Sea Res. I, 48, 237–267, doi:10.1016/S0967-0637(00)00059-5, 2001.

Varela, R. A., Roson, G., Herrera, J. L., Torres-Lopez, S., and Fernandez-Romero, A.: A general view of the hydrographic and dynamical patterns of the Rias Baixas adjacent sea area, J. Mar. Sys., 54, 97–113, doi:10.1016/j.jmarsys.2004.07.006, 2005.

Wooster, W. S., Bakun, A., and Mclain, D. R.: Seasonal upwelling cycle along eastern boundary of North-Atlantic, J. Mar. Res., 34, 131–141, 1976.

Yaremchuk, M. I., Nechaev, D. A., and Thompson, K. R.: Seasonal variation of the North Atlantic Current, J. Geophys. Res., 106, 6835–6851, doi:10.1029/2000JC900166, 2001.